

Hierarchical Classifier Design for Airborne SAR Images of Ships*

L. Gagnon¹ and R. Klepko^{2†}

¹R&D Department, Lockheed Martin Canada,
6111 Ave Royalmount, Montreal, Quebec, H4P 1K6, CANADA

²Aerospace Radar and Navigation Section, Defence Research Establishment Ottawa,
3701 Carling Ave, Ottawa, Ontario, K1A 0Z4, CANADA

ABSTRACT

We report about a hierarchical design for extracting ship features and recognizing ships from SAR images, and which will eventually feed a multisensor data fusion system for airborne surveillance. The target is segmented from the image background using directional thresholding and region merging processes. Ship end-points are then identified through a ship centerline detection performed with a Hough transform. A ship length estimate is calculated assuming that the ship heading and/or the cross-range resolution are known. A high-level ship classification identifies whether the target belongs to Line (mainly combatant military ships) or Merchant ship categories. Category discrimination is based on the radar scatterers' distribution in 9 ship sections along the ship's range profile. A 3-layer neural network has been trained on simulated scatterers distributions and supervised by a rule-based expert system to perform this task. The NN "smoothes out" the rules and the confidence levels on the category declaration. Line ship type (Frigate, Destroyer, Cruiser, Battleship, Aircraft Carrier) is then estimated using a Bayes classifier based on the ship length. Classifier performances using simulated images are presented.

Keywords: Automatic Target Recognition, Ship Classification, Knowledge-Based Rules, Neural Networks

1. INTRODUCTION

Due to the increasing technological advance of airborne-based imaging sensors, design and implementation of automatic ship recognition systems are getting much interest in the scientific and engineering communities. Despite the fact that automatic ship recognition brings out interesting scientific challenges, still very few results are reported in the open literature (See, for instance, Refs. 1-8 and 14). Admittedly, many practical issues make automatic ship recognition a very complex problem, in particular for Synthetic Aperture Radar (SAR) imagery:

- uncontrolled environment
- variable 3-D image acquisition geometry and resolution
- image blurring due to target motion
- high noise level (speckle)
- dependence of radar scattering to ship orientation
- operator requirements (up the 1000 ships in database)
- difficulty of accessing real image data due to potential strategic interest

Various objects recognition techniques are being proposed in the open literature to handle SAR-based ship recognition¹⁻⁶. Zwicke and Kiss¹ uses a modified Mellin transform to extract angle-independent ship features from range-profile, Drazovich² et al. extract structural features (e.g. ship length, main structure position) to feed a Knowledge-Based (KB) system, Musman and Kerr³ also use a method based on superstructure location together with multi-frame analysis for ISAR images, finally

* SPIE Proc. #3371, conference "Automatic Target Recognition VIII", Orlando, 1998

† Current address: Nortel, Public Carrier Networks, Ottawa, Ontario, K1Y 4H7, CANADA

Further author information -

L.G.(correspondence): Email: langis.gagnon@lmco.com; WWW: <http://www.crm.umontreal.ca/~lgagnon>

Menon⁴, Bachmann⁵ et al. and more recently Osman⁶ et al. propose various Neural Network (NN) architectures to encode pixel intensity distribution.

The purpose of this paper is to give an overview of a SAR-based ship classifier under development at Lockheed Martin Canada (LM Canada) over the last 2 years in collaboration with University partners (Queens and Montreal Universities) and more recently under contractual R&D activities for the Defence Research Establishment Ottawa (DREO). These researches are part of the LM Canada R&D activities in airborne sensor fusion with targeted applications in maritime and coastal surveillance (LM Canada is the prime contractor for a new Spotlight SAR (SSAR) sensor to be mounted on the Canadian surveillance aircraft CP-140). The aim is to demonstrate the potential improvement that SAR imagery can provide for long-range target identification within a multi-sensor environment of an airborne Command and Control System (CCS).

Figure 1 gives a high-level description of the system LM Canada is currently studying (a more detailed description will be given in Section 2). To some extent, the classifier can deal with SAR (i.e. SSAR) as well as ISAR images. It performs hierarchical feature extraction and target declarations which will be fused (using evidential reasoning theory) with features and/or declarations from other imaging and non-imaging sensors⁹ (Electromagnetic Support Measures, Identification Friend or Foe, conventional radar, Forward Looking InfraRed camera, etc.). The hierarchical approach has numerous advantages:

- low technical risk due to the use of pattern recognition algorithms of increasing complexity
- easier system design refinement and upgrade
- incremental implementation
- easier and more efficient retraining procedures than for large classifiers

The ship nomenclature we use in this paper is based on the latest NATO Standardization Agreement¹⁰ 4420 for surface tracks and is reproduced in Figure 2. Line and Merchant are the 2 ship categories that we are concentrating on. Frigate, Destroyer, Cruiser, Battleship and Aircraft Carrier are the ship types for the Line category. We have not yet included capability to discriminate between Merchant ship types in our classifier. Ship class in Step 4 (Figure 1) actually refers to the generic ship name (e.g. Halifax-class Frigate) and is by far the most difficult and challenging part of the whole design.

2. DESIGN

The preliminary target detection step and the SAR antenna orientation are assumed to be performed with the help of the range-bearing information provided by the conventional radar mode. At the operator request, a potential ship target is imaged at high resolution using the SAR or ISAR modes. For now, we assume that the SAR image generator provides adequate platform and target motion compensations to assure minimal blurring effects in the image (otherwise, this can impose a severe limit in the classification performance). The resulting target image, along with the target-aircraft distance, the platform altitude and the target aspect angle (which could be acquired from a previous long tracking time), constitute the input data for the system.

In reference to Figures 1 and 3, here is a description of the main features of our SAR-based ship classifier.

Step 1: Target segmentation

Target segmentation from the ocean clutter is done in 2 steps: noise removal and merging of small regions. Noise removal is done column by column first, then row by row in order to remove linear strikes and artifacts caused by rotating ship antenna and/or SAR image generator defects. Noise mean μ and variance σ are estimated on the image border for each column/row assuming the target is centered in the image window. This is followed by a simple pixel intensity thresholding where thresholds have been set to $(\mu + 4\sigma)$ and $(\mu + 2\sigma)$ for columns and rows, respectively. Residual small non-connected clutter regions are further discarded if they are isolated and their spatial extent is above an empirically determined threshold. The resulting segmented image is binarized and sent to the ship centerline detection algorithm (Step 2).

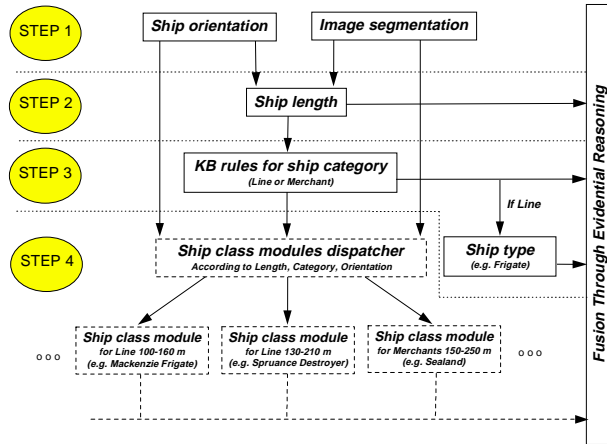


Figure 1: High-level description of the hierarchical ship classifier design

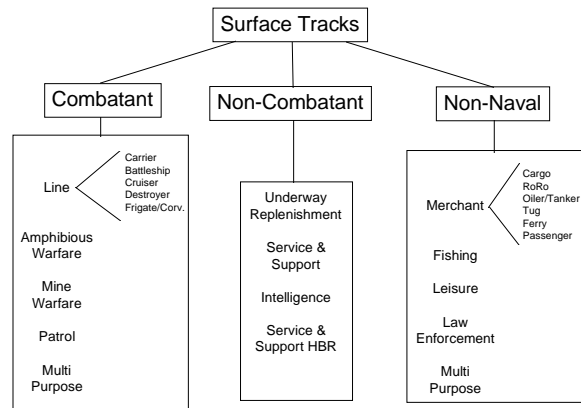


Figure 2: STANAG 4420 nomenclature for Surface Tracks

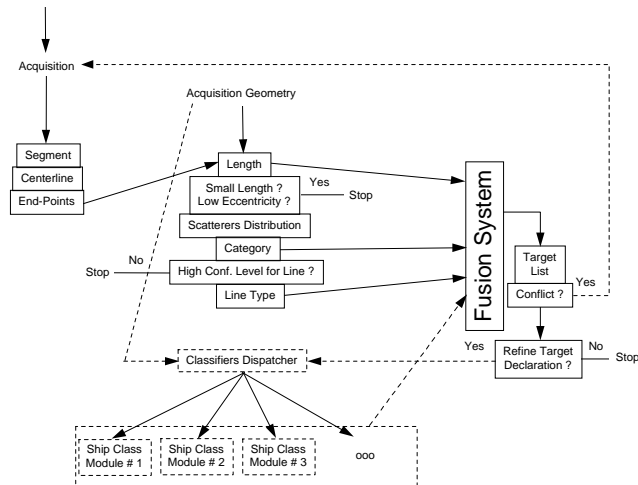


Figure 3: Low-level description of the hierarchical ship classifier design

Step 2: Ship length estimate, length and eccentricity tests

Ship length is a simple but very discriminating feature in ship type classification; especially for large Line ships. Ship length L is obtained by identifying the target's end-points. Following Musman³ et al., ship end-points can be obtained by estimating the ship center-line from the maximum peak of the Hough transform of the segmented image. This technique is more robust than a least-square-fit through the target or principal axes detection because a large amount of cross-range scatterer spreading in some images (especially ISAR) tend to bias the centerline estimation. The same is true if residual small clutter regions are present in the image. For instance, Figure 4 shows a portion of a (unclassified) RADARSAT ship image with a correct centerline detection in presence of a small residual target. The accumulator space of the Hough transform (right) shows the local maximum corresponding to the large (circle) and small (square) ships.

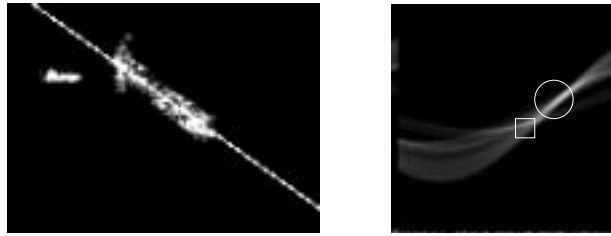


Figure 4: Example of correct ship centerline detection in presence of a small residual target (left). Accumulator space of the Hough transform (right) showing two local maxima which correspond to the large (circle) and small (square) ships.

Once ship end-points are determined, ship length can be calculated using either

$$L = \sqrt{l_{sr}^2 + l_{cr}^2} \quad L = l_{sr} / \sin|H| \quad (2.1a,b)$$

where l_{sr} and l_{cr} are the (slant)-range and cross-range ship length in meters measured on the SAR image (taking into account image resolution) and H is the ship heading angle (Figure 5). Equation 2.1a can be used only on SAR images for which cross-range resolution is known. In practice, SAR antenna depression angle is very low and thus aircraft altitude is not taken into account in the calculation of L .

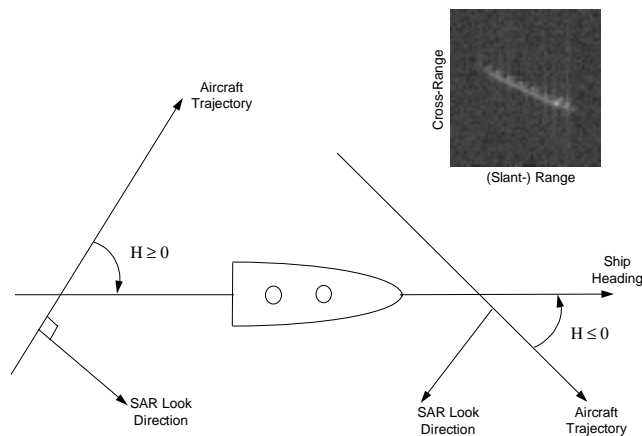


Figure 5: Geometry definition of ship heading and radar LOS

Length L represents a lower bound for the ship length because ships do not necessarily scatter energy along its entire length. In addition to computing the minimum ship length L , a maximum ship length is estimated based on two assumptions:

- ship scatters along at least $100L/(20+L)\%$ of its length (an empirically determined ratio)
- segmented target length is no less than 90% of the target length visible on the initial image

Maximum ship length is thus computed using $(20+L)/0.90$. In addition, error on aspect angle H should be taken into account while using Eq. 2.1b, typically $\pm 5^\circ$ from a Track-While-Scan system. Here we assume H is known exactly. When cross-range resolution as well as ship heading are known, both ship length range estimates from Eqs. (2.1) are combined to minimize risk of error. In our test, we take the minimum and maximum ship lengths of the union of both ship length intervals.

Following the target length estimate, 2 screening steps are performed. First, if the minimum target length is larger than 80 m, then the original image is sent to the first target classification step (Step 3); otherwise it is labeled as small ship and not analyzed further (our current ship data-base does not contain small ships yet). Besides, a small ship declaration can also be caused by a failure of the segmentation or of the ship end-points detection steps. Second, knowing the ship end-points allows to delimit a ROI around the principal target in the segmented image. The eccentricity of this target is calculated and serve as a screening step to discard objects that are not enough elongated due to possible image artifacts or blurring. In addition, ships are always best recognized, even for humans, from broadside or plan views. In our implementation, targets having eccentricity lower than 3.0 are not processed further.

Step 3: Ship category and ship type declarations

Step 3 is the first target classification step in the hierarchy. It provides (1) a high-level identification declaration of the ship category, that are Line, Merchant or Unrecognized ship and (2) a medium-level declaration of Line ship type.

Ship category

The category declaration is based on the gross spatial distribution of ship radar scatterers. Line ships have large structures, thus radar scattering, mainly concentrated in the middle part of the ship while Merchant ships scatter mainly from the ship end-regions. The discrimination is based on the number of important scatterers (e.g. the 10% most intense pixels in the image) in 9 equal sections of the segmented target. Separating lines between various sections are perpendicular to (1) the (slant-) range axis for ISAR image and (2) the ship centerline for SAR images; the latter requiring an estimate of the widthwise ship apparent axis.

Different number of sections were tried, but not enough structural detail was defined with less than 9 and more resolution than was necessary to distinguish the general shapes was achieved with more than 9. Because of the limited availability of real and simulated image data, a set of 9-dimensional vectors simulating scatterer distributions has been generated and used to train and test a 3-layer back-propagation Neural Net (NN). To restrict the number of vectors while having a fair uniform sample distribution, we have limited the set to all combinations (with repetitions) of numbers 0, 4, 8, 12 and 16, in 9 entries and for which the sum of all entries is 40. This results in 16105 samples that are further normalized such that the sum of all entries is 1.0.

The NN is supervised by a set of 37 production rules (a kind of knowledge-based supervisor) previously developed by DREO¹¹ and improved at LM Canada to include evidence measures. These rules were created by browsing through the entire Jane's Fighting Ships¹² and Jane's Merchant Ships¹³ references to see what the variety of superstructures looked like and what is the general appearance of each category. Here is an example of a production rule:

If the first four ship sections with more radar scattering are 6, 7, 8 and 9 (in any ordering), and section 6 is not the first or second, and section 7 is not the first then there is evidence (with empirically determined measures) that the ship is a Line (10%), a Merchant (80%) or non-recognized (10% ignorance)

The number of rules increases exponentially with the number of analyzed ship sections, which constitutes another reason why we have limited number of ship sections to 9.

The advantage of training a NN with rules rather than using the rules themselves to identify the target is twofold. First, the NN "smoothes out" the rules (i.e. artificially increases the number of rules) which makes them less sensitive to small

distribution variations along the 9 ship sections (the rules are not exhaustive). For instance, it prevents a category declaration switching from Merchant to Line with only one scatterer difference within one section. Second, it provides a mapping between the infinite possibilities of scatterers distributions and the assigned evidences (confidence level) for propositions. In our implementation, the confidence level for each ship category proposition (including ignorance) has been empirically set to $0.94 O_{cat} + 0.02$, where O_{cat} is the normalized confidence level of the corresponding NN output. This is to avoid limiting the adaptivity of the subsequent fusion algorithm by a 0 % confidence level on the ignorance.

According to the KB supervisor, from the 16105 vectors, 8100 were associated to Line ships, 2939 to Merchants and 5066 were not recognized. These ratios are typical of a military surveillance mission for the CP-140.

Line ship type

If the confidence level on a Line declaration is high enough (lets say > 50%), then an estimate of the Line ship type is initiated. This is performed by a Bayes classifier based on the Frigates, Destroyers, Cruisers, Battleship and Carriers length distributions. Ship lengths have been obtained by browsing Jane's Fighting Ships¹² and their probability density distributions approximated by Gaussians (Figure 6).

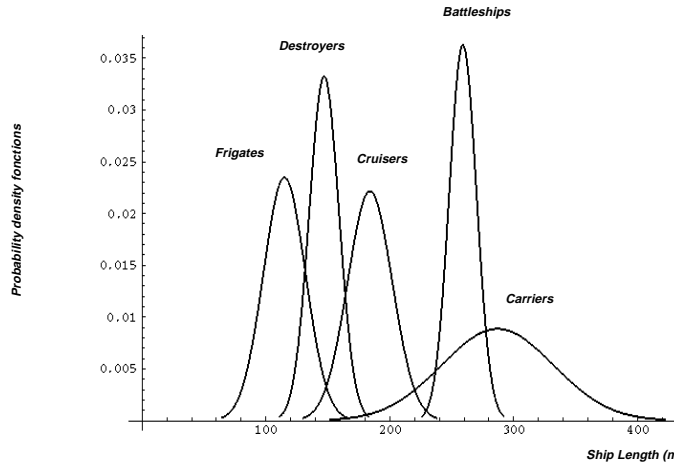


Figure 6: Probability density distribution model for Line ship length

Given a ship length range evaluated in Step 2, one calculates the mean *a posteriori* type probability $P_{avg}(t|s)$ that a ship s belongs to type t by averaging the standard Bayes rule over the entire ship length range,

$$P_{avg}(t|s) = \underset{\text{length range}}{\text{Avg}} \left(\frac{p(s|t)P(t)}{p(s)} \right) \quad p(s) = \sum_i p(s|t_i)P(t_i) \quad (2.2a,b)$$

where $p(s|t)$ and $P(t)$ are the Gaussian probability density distribution and the *a priori* probability of type t , respectively. The *a priori* probability $P(t)$ depends on the context and could be set by the radar operator prior the mission. In our tests, we assume equal probability for the 5 Line ship types. Mean *a posteriori* type probabilities are re-normalized, in order that their sum is unity, and multiplied afterwards by O_c . The resulting number O_{type} serve to set the confidence level on ship type declarations which have been empirically chosen as $0.86 O_{type} + 0.02$. Note that the Merchant and Unrecognized categories confidence levels are also renormalized using $0.86 A + 0.02$, where $A = \{O_{Merchant}, O_{Unrecognize}\}$.

Step 4: Ship class declaration

If a more accurate target identification is required, that is, ship class (e.g. Mackenzie-class frigate, Belknap-class cruiser) and the confidence level on the ship category is sufficiently high, then Step 4 should be initiated.

Obviously, this necessitates much more sophisticated classifiers in order to discriminate between ship classes (it also requires high-quality and high-resolution images with minimal blurring due to target motion). Rather than training a huge classifier that would most probably lead to convergence problems, we are considering a modular approach consisting of many small dedicated classifiers, each of them being specialized to recognize a subset of the ship database under a small viewing angle range (Figures 1 and 3). This approach is advantageous for large databases as it avoids training a large classifier when a new ship is entered in the database (a typical ship database for surveillance activities might contain up to 1000 ships, imaged at 360 different aspect angles and 10 depression angles, namely 3.6 millions of images). During the recognition process, only modules corresponding to the acquisition geometry, ship length range and probable ship category or types would be fired. This information can be obtained from Steps 2 and 3 as well from the fusion system which has the capability of providing a list of the most probable target identifications.

SAR and ISAR images have to be processed differently in Step 4. Recognition should be done from the range-profile for ISAR images while the entire image can be used for SAR. This work is under progress but 2 module architectures have been tested by our University partners for SAR images (other interesting ISAR-based ship classifiers have been reported in the open literature^{3,4} and at least one of them is known to be operational⁴). One is based on the Principal Component Analysis¹⁴ “à la MIT” and the other is a kind of multi-resolution back-propagation NN⁵. The later provides good results on a small set of simulated images but tests on the modules interconnection and using a large database still have to be done. The implementation of this part is not yet completed and we will not go further into it here.

3. TESTS ON SIMULATED IMAGES

Use of a computer-based ship SAR/ISAR image simulation facility enables an extensive database of images to be generated. Numerous images can be produced for various combinations of ship motions and orientations. This simulation facility provides a very cost effective method for acquiring radar images when compared to the alternative methods of acquiring real images, using either full sized vessels or scaled down ship models. It also enables extensive testing of automatic ship classification algorithms.

We use a CAD modeler and a radar scattering simulator developed by London Research and Development for DREO¹⁵. It is assumed that the ship is a rigid body (no flexion or vibration of hull) which can be modeled as untextured plates, corners and corner cubes. The CAD modeler uses a 2-dimensional block-based method to generate a numerical representation of ships structures, as it appears above the waterline. Our database contains the 46 ships listed in Table 1. The SAR/ISAR simulator uses a physical optics approximation for the RCS estimation. Artificial image degradation algorithms (blurring and speckle noise) have been added to the simulator in order to generate images of more realistic appearance (e.g. texture).

Category	Type	Class	#
Lines	Frigates	Boxer, Oliver Hazard Perry, Knox, Bremen, Amazon, Grisha, Krivak, Mackenzie, Ste-Croix, Terranova, Mirka	11
	Destroyers	Adams, Coontz, Spruance, Iroquois, Kotlin Sam, Udaloy, Sovremenny	7
	Cruisers	Belknap, Longbeach, Virginia, Sverdlov/Dzerzhinski, Kara, Ticonderoga, Kresta	7
	Battelships	Kirov, Moskva	2
	Carriers	Kiev, Nimitz, Invincible, Tarawa	4
Merchants	Cargos	Donato Marmol, Geestbay	2
	Containers	Sealand Freedom, Sydney Express	2
	Bulk Carriers	Farland, Radnik	2
Others	Supply	Sacramento, Preserver, Boris Chilikin, Ivan Rogov, Ugra	5
	Tug	John Ross	1
	Navigation	Sir William Alexander	1
	Research	Quest	1
	Trawler	Trawler	1

Table 1: Ship database

In the following, we present classifier performances for simulated SAR images only, and under radar, target and aircraft simulation parameters given in Table 2.

Target Distance (km)	Aspect Angle (H) (°)	(Slant-) Range Resolution (m)	Cross-Range Resolution (m)	Aircraft Altitude (m)	Aircraft Velocity (km/s)	Radar Frequency (GHz)
100	$\pm 30, \pm 80$	0.75	2	3000	0.15	10

Table 2: Simulation parameters used for the tests

Figure 7 shows 2 examples of processed SAR images: the upper part is the actual input image, the middle part shows the ROI, the ship centerline and the widthwise ship axis, and the bottom part gives the most intense pixels from which ship category is determined. Segmentation and centerline detection are sensitive to ship aspect angle because of the different radar scattering signature.

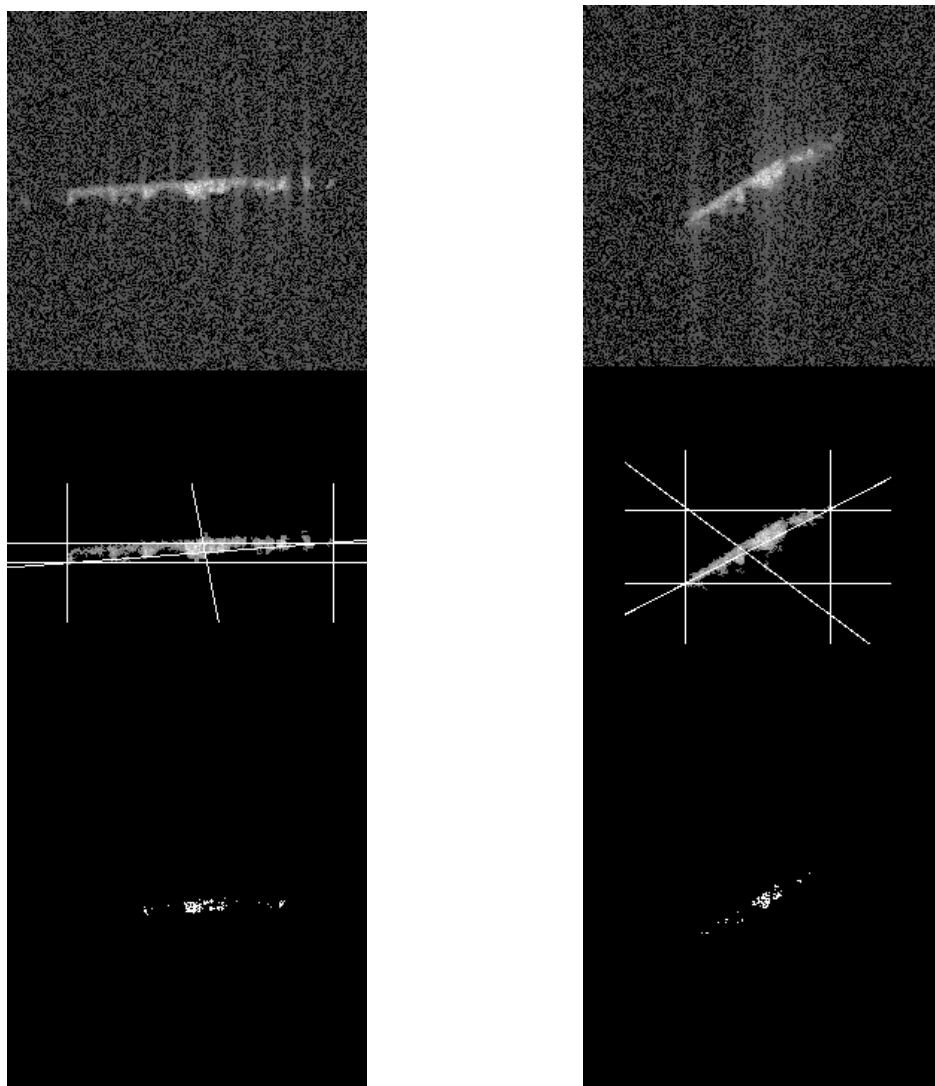


Figure 7: Examples of processed images (see text for details)

Tables 3-5 gives the confusion matrices for ship category and type declarations cumulated over the 4 ship headings (Table 2). The “Rejected” column refers to the number of images which did not pass the minimum ship length or eccentricity tests. For the category (Table 3) and 1-proposition type (Type 4) declarations, the winning declaration is the one which has the highest confidence level. For the 2-proposition type (Type 5) declarations, the winner is the one corresponding to the sum of the two highest confidence levels. Here are few remarks about results depicted in Tables 3-5:

- A rejected image cannot really be considered as a totally incorrect declaration
- An “Unrecognized” declaration cannot really be considered as a totally incorrect declaration for Line and Merchant ships because the KB rules that served to train the NN are not exhaustive
- 17% of the images have been rejected (14% for Lines, 14% for Merchants and 31% for Others)
- 4% of Lines have been incorrectly classified (Lines declared as Merchants)
- 50% of Merchants have been incorrectly classified (Merchants declared as Lines)
- Clearly, the system is more robust to recognize Line ships than Merchants
- However, 43% of Merchants and Others have been declared as Lines while 11% of Lines have been declared as Merchants or Others. This can be interpreted as a tendency of the system to overestimate the target threat; which is not necessarily a drawback for military surveillance platforms
- Table 4 shows that the system is not very robust for 1-proposition ship type declarations (45% for Frigates, 50% for Destroyers, 68% for Cruisers, 37% for Battleships and 42% for Carriers)
- However, 2-propositions ship type declarations (Table 5) are more faithful (77% for Frigates, 96% for Destroyers, 82% for Cruisers, 62% for Battleships, 75% for Carriers). Even though more generic, such declarations are still very useful within our current sensor fusion environment

	Total	Rejected	Sub-Total	Lines	Merchants	Unrecognized
Lines	124	17	107	95	4	8
Merchants	28	4	24	12	4	8
Others	32	10	22	8	6	8

Table 3: Confusion matrix for ship category declarations

	Total	Rejected	Sub-Total	F	D	C	B	A	MvU
Frigates	44	13	31	14	13	-	-	-	4
Destroyers	28	-	28	3	14	11	-	-	-
Cruisers	28	-	28	-	5	19	-	-	4
Battleships	6	-	8	-	-	3	3	1	1
Air. Car.	16	4	12	-	-	4	-	5	3

Table 4: Confusion matrix for 1-proposition ship type declarations

	Total	Rejected	Sub-Total	FvD	DvC	CvB	BvA	CvA	MvU
Frigates	44	13	31	24	3	-	-	-	4
Destroyers	28	-	28	7	20	-	-	1	-
Cruisers	28	-	28	1	12	1	-	10	4
Battleships	6	-	8	-	1	1	4	1	1
Air. Car.	16	4	12	-	-	-	4	5	3

Table 5: Confusion matrix for 2-propositions ship type declarations

For complementary information, Table 6 gives the detailed ship declarations for the data subset $H = +80^\circ$. Confidence levels for ship type do not sum to 100% because of the residual weighted confidence levels for Merchant and Unknown categories (not shown). First column gives the ship class and the real ship type and length (in meters). Second column is the estimated ship length range. Columns 3 to 10 gives the confidence levels of the various category and type declarations.

	Length	L	M	Unrecog.	F	D	C	B	Air. Car.	Comments
adams (D-133)	131-169	84	7	9	12	52	17	2	2	
amazon (F-117)	80-112	83	7	10	76	2	2	2	2	
belknap (C-167)	136-174	85	7	8	8	49	24	2	2	
boxer (F-145)	142-182	49	9	42	4	23	22	2	2	
bremen (F-130)	108-143	68	5	26	42	22	3	2	2	
chilikin (O-162)	158-198	2	87	11	-	-	-	-	-	
coontz (D-156)	131-168	85	7	8	13	53	16	2	2	
donatto (M-145)	120-156	3	82	15	-	-	-	-	-	
farland (M-272)	253-306	3	78	20	-	-	-	-	-	
geestbay (M-159)	151-192	7	33	60	-	-	-	-	-	
grisha (F-73)	69-100	45	9	46	41	2	2	2	2	Small length
invinc (A-206)	184-228	83	7	10	2	2	58	3	20	
irogov (O-159)	155-197	6	50	44	-	-	-	-	-	
iroquois (D-130)	109-144	83	6	10	49	28	3	2	2	
jross (O-95)	74-105	51	11	38	-	-	-	-	-	Small length
kara (C-174)	167-209	19	17	64	2	3	16	2	3	
kiev (A-270)	260-312	52	9	39	2	2	2	16	33	
kirov (B-248)	230-279	65	9	26	2	2	3	40	21	
knox (F-133)	124-161	68	5	27	18	42	7	2	2	
kotlin (D-126)	123-159	80	6	15	23	48	7	2	2	
kresta (C-158)	148-189	83	9	8	3	29	46	2	3	
krivak (F-122)	105-141	33	46	21	22	10	2	2	2	
longbeac (C-220)	200-247	6	39	55	2	2	4	3	3	
mckenzie (F-112)	76-107	68	5	27	63	2	2	2	2	Small length
mirka (F-81)	71-101	84	7	9	77	2	2	2	2	Small length
moskva (B-197)	145-186	4	11	85	2	3	3	2	2	
nimitz (A-332)	36-63	47	9	44	43	2	2	2	2	Bad segment.
perry (F-135)	117-153	75	8	17	31	38	4	2	2	
preserve (O-172)	132-170	81	8	11	-	-	-	-	-	
quest (O-77)	75-106	7	45	48	-	-	-	-	-	
radnik (M-189)	179-223	21	12	67	-	-	-	-	-	
sacramen (O-241)	235-286	5	50	44	-	-	-	-	-	
sealand (M-227)	199-244	80	7	13	-	-	-	-	-	
sirwalex (O-69)	62-92	76	7	17	-	-	-	-	-	Small length
sovrem (D-155)	151-191	84	6	9	3	26	51	2	3	
spruance (D-171)	166-208	83	6	11	2	7	67	2	6	
stcroix (F-112)	81-113	3	83	14	3	2	2	2	2	
sydney (M-210)	207-252	85	7	9	-	-	-	-	-	
tarawa (A-249)	252-302	9	30	61	2	2	2	5	5	
terranova (F-113)	76-108	61	5	35	56	2	2	2	2	Small length
ticonder (C-171)	157-197	72	7	21	2	15	51	2	4	
trawler (M-145)	38-65	3	67	30	-	-	-	-	-	Small length
udaloy (D-158)	141-181	85	7	8	5	41	35	2	3	
ugra (O-141)	130-168	85	7	8	-	-	-	-	-	
virginia (C-178)	156-198	85	7	8	3	18	60	2	4	
zerzinsk (C-210)	174-217	85	7	8	2	3	69	2	10	

Table 6: Detailed ship length estimation (meters) and confidence level declarations (%) for data subset $H = +80^\circ$

4. DISCUSSION

This paper presents the status of the SAR/ISAR-based ship classifier currently developed at LM Canada. The classifier design is based on a hierarchical approach that performs incremental feature extraction and target declarations in order to feed a multi-sensor fusion system developed at LM Canada under previous naval contracts. This approach offers a good trade-off between system complexity (efficiency) and time consuming process to create a test-bed. The system is currently able to provide ship category and ship type declarations for a large subset of military and merchant ships along with confidence levels. The processing time has been kept very low by avoiding complex algorithms; ship centerline detection is actually the most CPU consuming part with 5-15 seconds on a Pentium 133. Neural network training time is of course very much time consuming but this is done off-line.

Although the current system comes up to our main expectations, many aspects could be improved and are planned to be addressed in the future:

- More refined production rules are necessary for improving the category discrimination, especially between Merchants and Lines, and also between Supply (currently part of the "Unrecognized" category) and Merchant ships.
- More accurate ship length range estimate would help in discriminating between Line ship types. High quality images will provide a more faithful target segmentation and, consequently, a smaller ship length error.
- Automatic classification of Merchant ship types is a quite difficult task because not obvious to identify the right set of discriminating features. Maybe a different approach has to be envisaged.
- The ultimate performance of the classifier depends upon how accurately real ship SAR/ISAR images can be duplicated by a simulator. Fortunately, classification performance of Step 3 should be minimally affected by the image quality as only gross radar returns are considered and no training step on real or simulated images is required. This is not the case however for Step 4.
- In its current state, the CAD modeling procedure has its limitations, namely, the inability to represent sloped or curved surfaces, as well as, overhanging structures. A polygon-based modeling procedure would be more accurate, at the expense of increasing time consuming process to create the CAD models.
- The physical optics approximation is the easiest way to implement radar images simulation, requires less computations, but probably gives the least accurate results. Other popular RCS estimation techniques include geometrical optics, geometrical theory of diffraction and uniform theory of diffraction¹⁶. The geometrical optics technique fails when the radius of curvature at a point of scattering is infinite. Thus, flat plates or cylinders cannot be treated successfully. This problem can be avoided by physical optics approximations. However, this approach is valid only if the scatterer is sufficiently large and the scattering direction is not beyond five sidelobes of the specular direction (i.e. the main scattering lobe). Otherwise, the scattering power is underestimated. A better approximation, in this case, is the geometrical theory of diffraction. However, this technique does not account for transition regions, such as those in the radar shadow and reflection boundaries. It also fails to compute finite RCS values at scattering surfaces created by reflections from curved surfaces (i.e. caustics). A more complete and accurate, yet more complex, extension to the theory of diffraction, is the uniform theory of diffraction.
- There are still many open issues regarding the interconnection between the different classifier modules in Step 4. It is not yet clear, for instance, to what extent should the modules overlap in order to minimize the uncertainties in the declaration.
- Confidence levels are currently based on empirical evidence and *a posteriori* Bayesian probabilities to a cluster and do not yet take into account the global system performance nor the image quality.
- The Fusion System could eventually provide feedback to the image-based target identifier in order to help orienting the target identity and/or improving the declaration levels.
- The number of ships in our database should be increased to at least 100-200 ships in order to have a better performance evaluation.
- Tests on real data have been performed and give very encouraging results. However, we cannot report them in this unclassified paper.

5. ACKNOWLEDGEMENTS

This work is supported in part by the Canadian Department of National Defence (DND) under Contract #W7701-6-4081. L.G. acknowledges Steve Blostein and Hossam Osman from the Department of Electrical and Computer Engineering at Queens University (Kingston, Ontario) for their contribution to this work through a University/Industry grant from the Natural Science and Engineering Research Council (NSERC) of Canada (#661-100-94).

6. REFERENCES

1. P. E. Zwicke, I. Kiss Jr., "A New Implementation of the Mellin Transform and its Application to Radar Classification of Ships", *IEEE Trans. Pattern Anal. Machine Intell.* **PAMI-5**, pp. 191-198, 1983
2. R. J. Drazovich, F. X. Lanzinger, T. O. Binford, "Radar Target Classification", *Proc. IEEE PRIP '81*, pp. 496-501, 1981
3. S. Musman, D. Kerr, C. Bachmann, "Automatic Recognition of ISAR Ship Images", *IEEE Trans. Aerospace Electronic Systems*, Vol. 32, pp. 1392-1403, 1996
4. M. Menon, "An Automatic Ship Classification System for ISAR Imagery", *SPIE Proc. #2492*, pp. 373-388, 1995
5. C. M. Bachmann, S. A. Musman, A. Schultz, "Lateral Inhibition Neural Networks for Classification of Simulated Radar Imagery", *IEEE International Conference on Neural Networks*, Vol. 2, p. 115-120, Baltimore, 1992
6. H. Osman, S. Blostein, L. Gagnon, "Classification of Ships in Airborne SAR Imagery Using Backpropagation Neural Networks", *SPIE Proc. #3161*, pp. 126-136, 1997
7. F. Sadjadi, J. O'Sullivan, "Periscope Video Ship Classification", *SPIE Proc. #2756*, pp. 46-52, 1996
8. R. N. Strickland, M. R. Gerber, "Estimation of Ship Profiles from a Time Sequence of Forward-Looking Infrared Images", *Opt. Eng.*, Vol. 25, pp. 995-1000, 1986
9. A. Jouan, L. Gagnon, E. Shahbazian, P. Valin, "Fusion of Imagery Attributes with Non-Imaging Sensor Reports by Truncated Dempster-Shafer Evidential Reasoning", submitted to FUSION98, Las Vegas, July 1998
10. *STANAG 4420: Display Symbology and Colours for NATO Maritime Units*, Edition 2, NATO Unclassified
11. R. Klepko, "Automatic Pattern Classification of Airborne SAR Images of Ships", *DREO Report #1283*, Ottawa, 1995 (DND Classified)
12. *Jane's Fighting Ships*, Edited by Richard Sharp, Jane's Information Group, London, 1996
13. *Jane's Merchant Ships*, Edited by David Greenman, Jane's Information Group, London, 1996
14. V. Gouaillier, L. Gagnon, "Ship Silhouette Recognition Using Principal Components Analysis", *SPIE Proc. #3164*, pp. 59-69, 1997
15. J. K. E. Tunaley, J. B. A. Mitchell, "Classification of SAR Images of Shipping and Simulation of ISAR Images of Ships", London Research and Development, *DREO Report for Contract #13SV.97714-4-2588*, 1985
16. E. F. Knott, J. F. Shaeffer, M. T. Tuley, *Radar Cross Section: Its Measurement and Reduction*, Artech House, Dedham, Mass. 1985.